

# Structural internal deterioration detection with motion vector field image analysis using monocular camera

Hiroshi Imai, Masahiko Ohta and Kazuhito Murata  
 Information and Media Processing Laboratories, NEC Corporation  
 1753 Shimonumabe, Nakahara-ku, Kawasaki, Kanagawa 211-8666, Japan

## Abstract

This paper describes a non-contact structural internal deterioration measurement method. The method can detect the internal deterioration by separating in-plane displacements and out-of-plane displacements from motion vector field images using a monocular camera.

## 1. Introduction

Accidents caused by the aging of social infrastructures such as bridges have been major social issues in the world. In conventional inspection such as visual inspection and hammering test by human, scaffoldings have to be set up so that inspectors approach near the infrastructures. This kind of inspection imposes financial issues such as equipment costs, labor costs and opportunity loss through traffic stop. Furthermore, there is a problem of variation in inspection accuracy. In this background, image sensing is a convincing option for material condition measurement methods [1,2].

This paper describes a non-contact structural internal deterioration measurement method which discovers the deterioration from remote at low cost. The method uses motion vector field images which are acquired by digital image correlation. This paper also describes a method that can separate in-plane displacements and out-of-plane displacements with a monocular camera.

## 2. Stress fields detection using digital image correlation

Figure 1 shows mechanical characteristics of deflected beams according to internal deteriorations (Normal, Crack, Peeling and Cavity). Motion vector field images which are captured from the bottom of the beam represent stress fields. The stress fields (displacements between frames in motion picture) are calculated by digital image correlation with parabola fitting sub-pixel interpolation.

## 3. Internal deteriorations detection

Figure 2 shows displacements contour line graphs of each internal deterioration state. In this experiment, we use a urethane beam (length: 130mm, width: 100mm, thickness: 30mm, Young's modulus: 4MPa) with a load of 130gf (1.27N) and a monochrome camera (lens focal length: 8mm, object distance: 300mm and actual pixel resolution: 80µm/pixel). In the crack sample, X displacements of the crack portion slope are gentle compared with normal portion. In the cavity sample, Y displacements appear in cavity portion. In the peeling sample, X displacements are constant in peeling portion. Thus, by observing these features of displacements, the type of internal deteriorations were successfully discriminated.

Figure 3 shows temporal displacement characteristics in the case where the beam is applied an impulse. Cavity portions transform with delays and their amplitudes are small compared with normal portions. By using spatial and temporal displacement characteristics in combination, we confirmed that discrimination accuracy was improved.

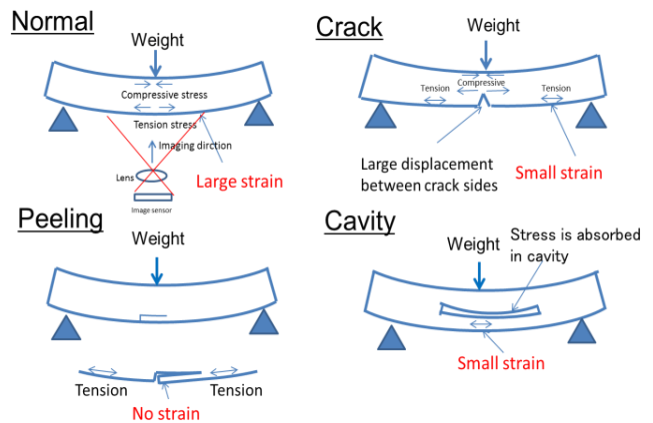


Figure 1. Mechanical characteristics of deflected beams.

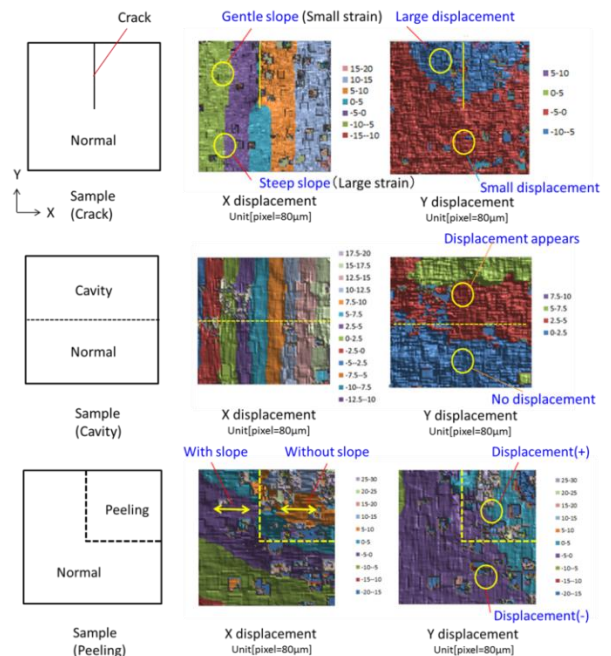


Figure 2. Displacements contour line comparison of each internal deterioration state.

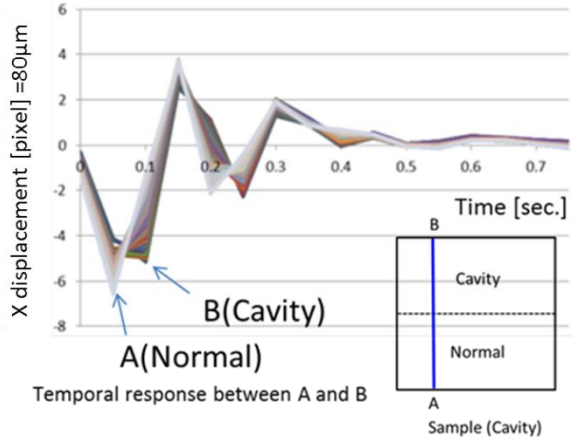


Figure 3. Temporal displacement characteristics.

#### 4. In-plane/out-of-plane displacements separation in the case of the presence of beam deflection

Figure 4 (a) shows the relationship between in-plane displacements and out-of-plane displacements with a monocular camera. Surface displacements, which correspond to the in-plane displacements in image plane, appear when a load is applied to the beam and internal deteriorations are detected (Figure 4 (b) shows the case of the crack opening).

However, out-of-plane displacements appear in the case where the beam moves along the optical axis due to deflection of it as shown in Figure 5 (a). In the case where large out-of-plane displacements add to in-plane displacements, it is difficult to separate in-plane displacements and out-of-plane displacements from measured displacements as shown in Figure 5 (b).

To separate these displacements, we propose two separation methods:

(Method 1) obtain out-of-plane displacements  $\delta_i(x)$ ,  $\delta_i(y)$  using deflection value  $\delta$  based on formula 1. Here, the deflection value  $\delta$  is measured with another distance measurement means (such as mechanical gauge, laser rangefinder, etc. ).

$$\begin{cases} \delta_i(x) = \left(\frac{1}{L-\delta} - \frac{1}{L}\right) xf \\ \delta_i(y) = \left(\frac{1}{L-\delta} - \frac{1}{L}\right) yf \end{cases} \quad (1)$$

Where,  $x$ ,  $y$  are coordinates in object.

(Method 2) estimate out-of-plane displacements from motion vector field analysis. In the case where structure surface is regarded as substantially a plane, the sizes of displacement vector  $R_{ref}(x_i, y_i, k)$  are given by:

$$R_{ref}(x_i, y_i, k) = k\sqrt{x_i^2 + y_i^2} \quad (2)$$

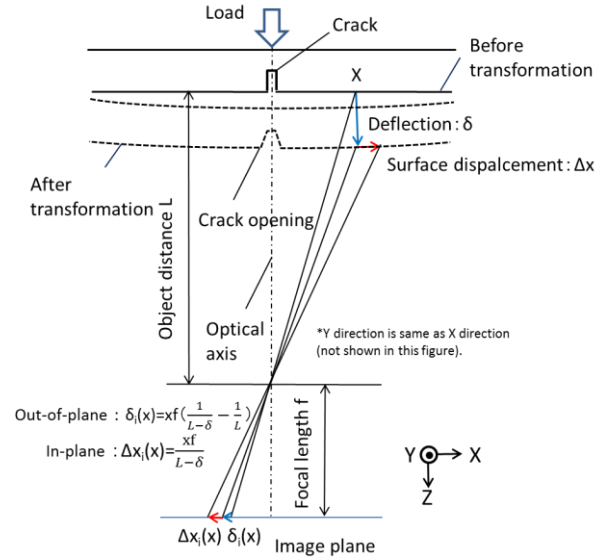
Where,  $x_i$ ,  $y_i$  are coordinates in image and  $k$  is a parameter which corresponds to object motion along the optical axis.

To estimate the out-of-plane displacements, the parameter  $k$  is calculated so that the function  $E(k)$  in formula 3 is to be the minimum.

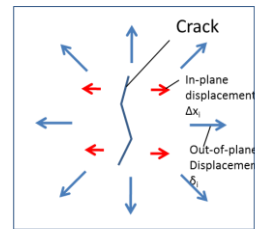
$$E(k) = \sum_{x_i, y_i} \{R_{mes}(x_i, y_i) - R_{ref}(x_i, y_i, k)\}^2 \quad (3)$$

Where,  $R_{mes}(x_i, y_i)$  are displacement size distributions which are given by:

$$R_{mes}(x_i, y_i) = \sqrt{\delta_i(x)^2 + \delta_i(y)^2} \quad (4)$$



(a) Relationship between In-plane and Out-of-plane displacement



(b) Displacement in image plane

Figure 4. Relationship between in-plane displacements and out-of-plane displacements with a monochrome camera.

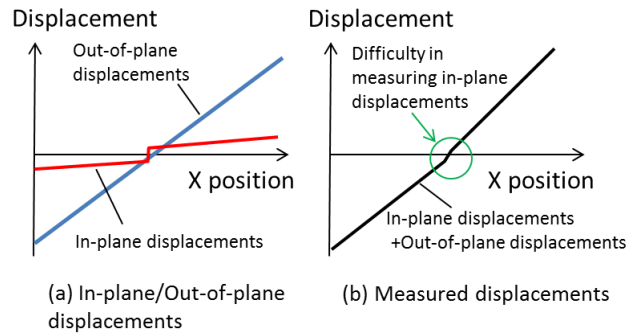


Figure 5. Characteristic relationship between in-plane displacements and measured displacements.

### 5. Experimental test using rigid plastic beam

Figure 6 shows the experimental set-up of rigid plastic beam. We use a ABS (Acrylonitrile butadiene styrene) resin beam (length: 400mm, width: 100mm, thickness: 10mm, Young's modulus: 4GPa) with a load of 6kgf(58.8N) and a monochrome camera (lens focal length: 12mm, object distance: 300mm and actual pixel resolution: 58µm/pixel). The beam is grooved on the center of its underside with a depth of 2mm.

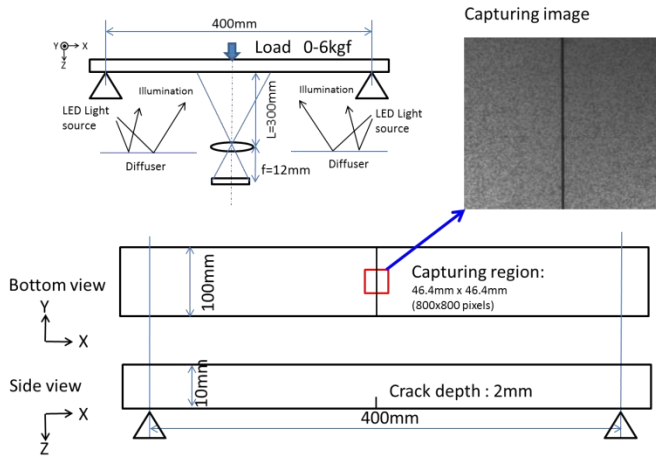


Figure 6. Experimental set-up of rigid plastic beam.

Figure 7 shows the measured displacement characteristics due to loading. Since the beam has surface deformation in the X direction, X displacement is slightly bigger than Y displacement. The in-plane displacement based on crack opening is hidden in out-of-plane displacement as shown in Figure 7.

To separate these displacements, first of all, we apply Method 1, which uses a measured deflection value of 4.3mm (measured by height gauge). With this method a crack opening of 0.3pixel (17.3µm in object plane) was detected in X displacements and Y displacements virtually disappear as shown in Figure 8.

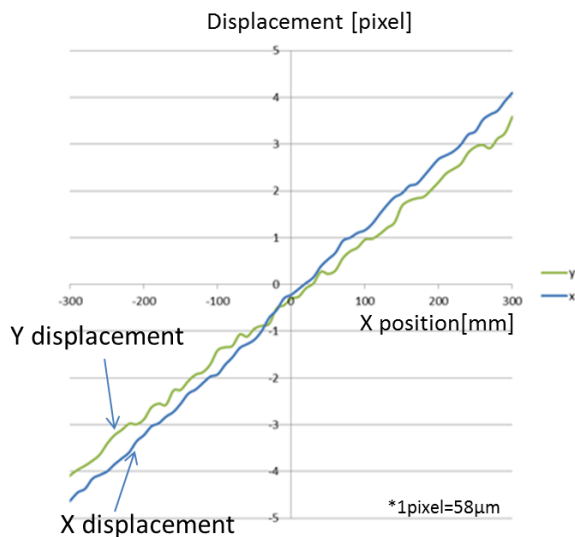


Figure 7. Measured displacement characteristics due to loading.

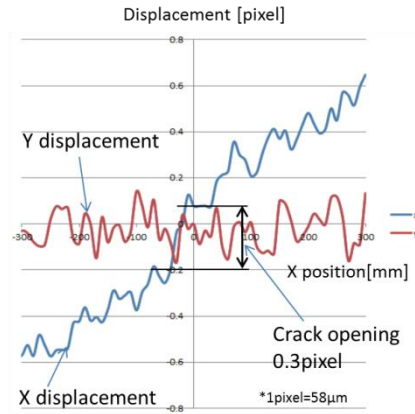


Figure 8. Separated In-plane displacements in X, Y direction.

Figure 9 shows displacement size distributions at each pixel in the image. Displacement size distributions  $R_{mes}(x_i, y_i)$  are similar to the function  $R_{ref}(x_i, y_i, k)$  in the case where in-plane displacements is very small compared with out-of-plane displacements as shown in Figure 10. In this figure it should be noted that the parameter  $k$  corresponds to the slope of the displacement size  $\Delta r$  against the radius from origin  $r$ .

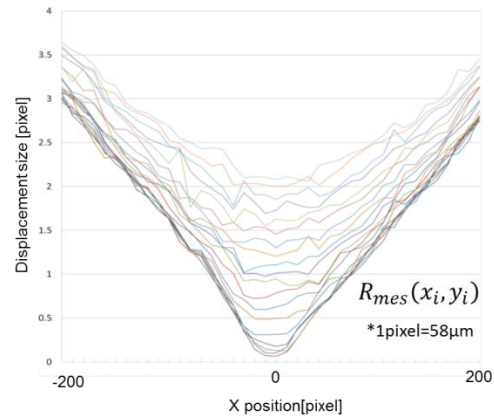


Figure 9. Displacement size distributions.

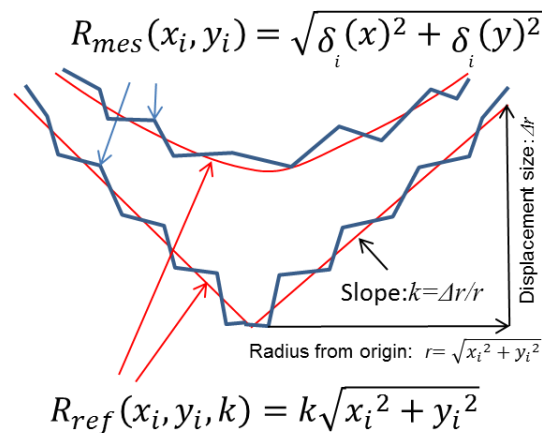


Figure 10. Displacement size distributions.

Thus, in this case, Method 2 can be applied for this experiment and by calculating a parameter  $k$  so that the function  $E(k)$  in formula 3 is to be the minimum with least squares method, a deflection value  $\delta$  can be estimated using the calculated parameter  $k$  as expressed by Formula 5. In this experiment, a parameter  $k$  value of 0.0145 (2.9pixels/200pixels) was calculated and we have successfully estimated a deflection value of 4.28mm which is equivalent to the measured value of 4.3mm in Method 1.

$$\delta = \frac{k}{k+1} L \quad (5)$$

Figure 11(a) shows a displacements separation result in the X direction with Method 1. This result is considered to be a value close to the reference value because of use of the measured deflection value. Figure 11 (b) shows a displacements separation result with the Method 2. This result shows a same crack opening of 0.3pixel which is equivalent to Method 1. Thus, we confirmed that Method 2 is also effective to separate both displacements. And both methods can be used for the structure internal deterioration.

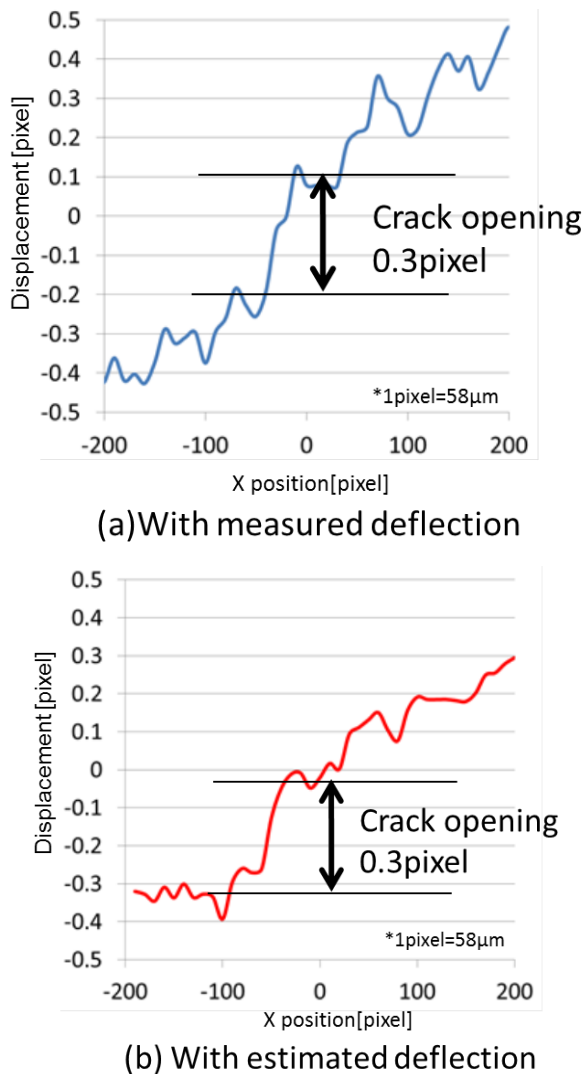


Figure 11. Displacements separation results.

Figure 12 shows a theoretical in-plane displacement simulation result using FEM (Finite Element Method) analysis. As shown in Figure 12, we confirm that the experimental results are reasonable in theoretical aspect of structural mechanics.

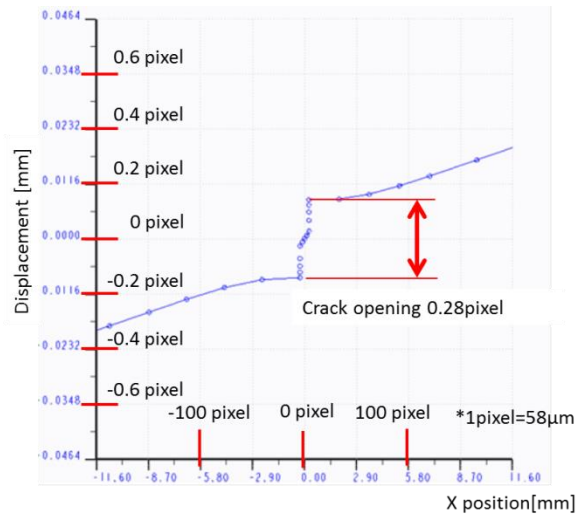


Figure 12. Theoretical in-plane displacement simulation result using FEM analysis.

## 6. Internal deteriorations detection in rigid material

Figure 13 shows the experimental set-up of rigid plastic beam with a cavity. We captured two regions of the beam. One is located on the center of the beam and the other is laterally offset from the center in the Y direction. In this experiment we applied Method 2 to separate out-of-plane displacements.

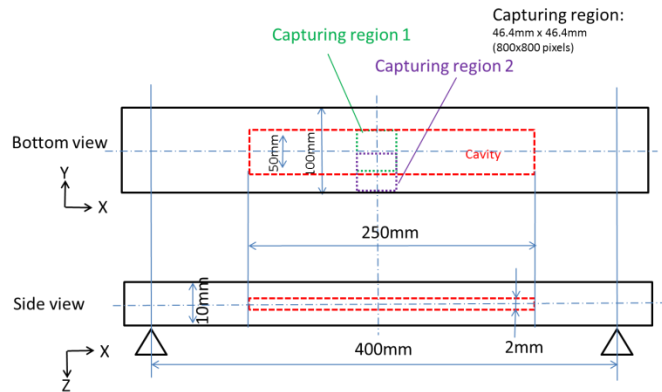


Figure 13. Rigid plastic beam with internal deteriorations of cavity.

Figure 14 shows a comparison result of in-plane displacements on the center of the beam (capturing region 1 in Figure 13) between experiment and FEM analysis. As shown in Figure 14, barrel shaped contour figures appeared in both result.

Figure 15 shows a comparison result of in-plane displacements on the offset position of the beam (capturing region 2 in Figure 13) between experiment and FEM analysis. On the edge of the cavity, the cavity portion slopes are gentle compared with normal portion as shown in Figure 15. By identifying these displacement characteristics, we also detect the cavity in rigid material.



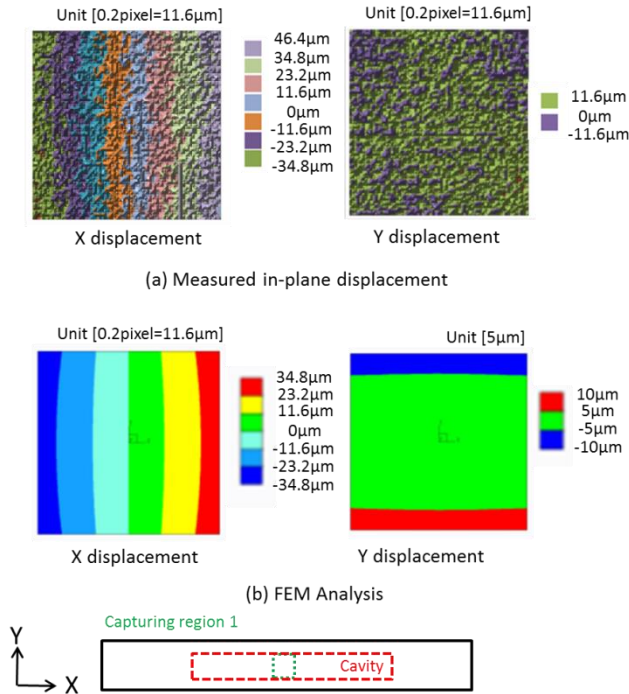


Figure 14. In-plane displacements in rigid plastic beam with internal deteriorations of cavity (Region 1).

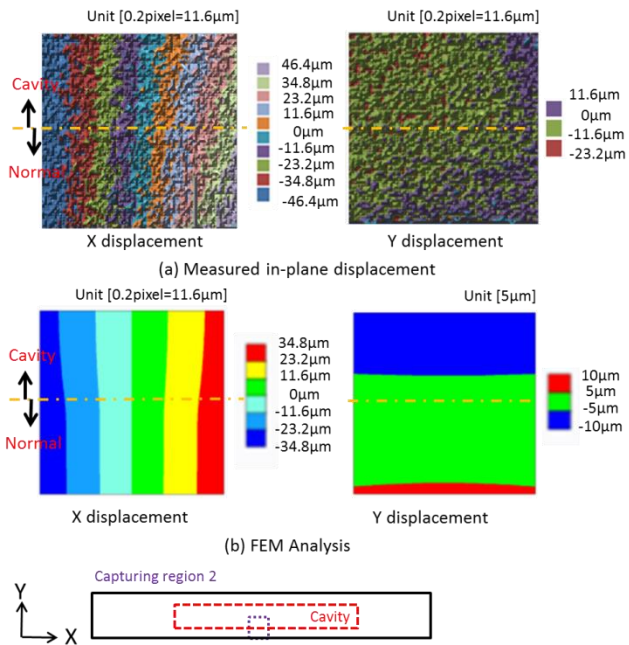


Figure 15. In-plane displacements in rigid plastic beam with cavity (Region 2).

## 7. Deflection measurement from out-of-plane displacement

The deflection value of beam also helps to detect the deterioration of structure such as bridges [3]. As mentioned the discussion of out-of-plane displacement, the amount of the deflection can be estimated with Method 2.

Figure 16 shows contour line graphs of measured displacement size distributions  $R_{mes}(x_i, y_i)$  which are given by formula 4. In the case of a heavy load of 6kgf, the slope of the displacement size against the radius from origin is 2.9pixels/200pixels whose estimated deflection is 4.28mm as show in Figure 16 (a). In the case of a light load of 130gf, the slope of the displacement size against the radius from origin is 0.044pixel/200pixels whose estimated deflection is 65μm (measured deflection with PSD-based displacement sensor, whose accuracy is  $\pm 5\mu\text{m}$ , is 70μm) as show in Figure 16 (b).

In figure 16 (b), 1 contour line of 0.02pixel can be observed. Thus, by using up to this displacement size step, a deflection measurement resolution of 30μm for object distance of 300mm, which corresponds to 0.5mm for object distance of 5m, can be promised. And the capturing region expansion allows the deflection measurement resolution to be improved.

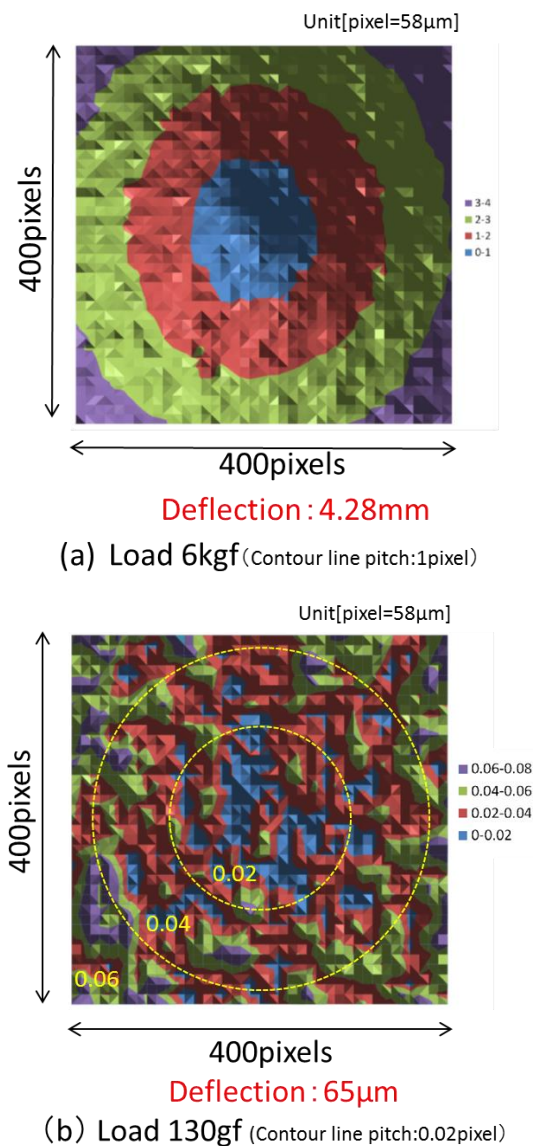


Figure 16. Displacement size distributions.

## 8. Conclusions

We have developed a non-contact structural internal deterioration measurement method which discovers the deterioration. The method can discriminate the type and degree of internal deterioration by observing surface displacements of structure and by separating in-plane/out-of-plane displacements using a monocular camera. Our proposed methods can also measure deflection simultaneously. Thus, it provides a non-contact remote infrastructure inspection system at low cost and it will solve the infrastructure inspection issues.

## References

- [1] Bing Pan et al. ,”High-accuracy 2D digital image correlation measurements using low-cost imaging lenses: implementation of a generalized compensation method”, Measurement Science and Technology vol.25 (2014) , 025001
- [2] Abe Davis et al. ,”Visual Vibrometry: Estimating Material Properties from Small Motions in Video” IEEE Conference on Computer Vision and Pattern Recognition (CVPR) 2015, pp.5335-5343
- [3] Satoru Yoneyama et al. ,” Bridge Deflection Measurement Using Digital Image Correlation with Camera Movement Correction” Materials Transactions, Vol. 53 (2012), No. 2 pp. 285-290

## Author Biography

*Hiroshi Imai received his BE degree in applied physics from Waseda University (1991) and his ME degree in information processing from Tokyo institute of Technology (1993). Since then he has worked in NEC Central Research Laboratories. His work has focused on the research of optoelectronics equipment, including optical sensing and display technologies. He is a member and a steering committee of the Optical Design Group (ODG) of the Optical Society of Japan (OSJ).*

*Masahiko Ohta received his BE(2005) and ME(2007) degrees in electronic engineering from The University of Electro-Communications respectively. Since then he has worked in NEC Central Research Laboratories. His work has focused on the development of optoelectronic systems based on optical sensing, image processing and display technologies.*

*Kazuhito Murata received his BE degree in mechanical engineering from Osaka Prefecture University (1990) and his ME degree in control engineering from Osaka University (1992). Since then he has worked in NEC Central Research Laboratories and Production Engineering Development Laboratories. His work has focused on the research, development and design of production system and process.*